# Supporting Information for the manuscript

## Metal-Organic Framework Nanosheets for Fast-Response and Highly Sensitive Luminescent Sensing of $Fe^{3+}$

Hui Xu,‡[a] Junkuo Gao,‡[b] Xuefeng Qian,[b] Jiangpeng Wang,[b] Huajun He,[a] Yuanjing Cui,*[a] Yu Yang,[a] Zhiyu Wang [a] and Guodong Qian*[a]

[a]*State Key Laboratory of Silicon Materials, Cyrus Tang Center for SensorMaterials and Applications, Department of Materials Science &Engineering,Zhejiang University, Hangzhou 310027, China. E-mail:gdqian@zju.edu.cn*

[b]*The Key laboratory of Advanced Textile Materials and Manufacturing Technology of Ministry of Education, National Engineering Lab for Textile Fiber Materials and Processing Technology (Zhejiang), College of Materials and Textiles, Zhejiang Sci-Tech University, Hangzhou 310018, China*

‡ *These authors have equal contribution to this paper.*

*Corresponding Authors. E-mail: cuiyj@zju.edu.cn, gdqian@zju.edu.cn

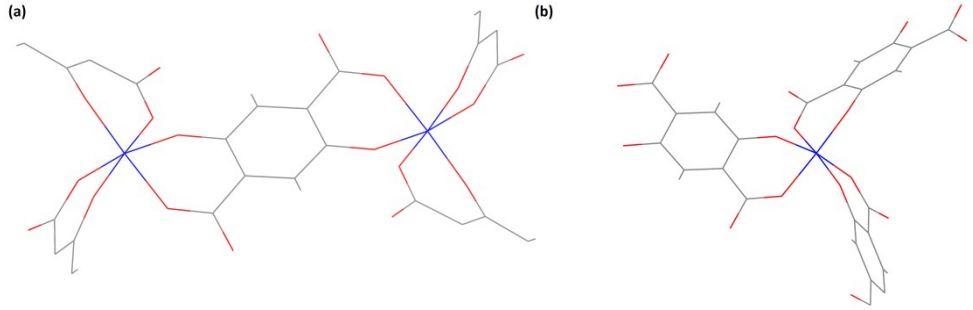


**Figure S1** X-ray single crystal structure shows the coordination mode of of **NTU-9** (a) coordination mode of the ligand DOBDC (b) coordination mode of $Ti^{4+}$.

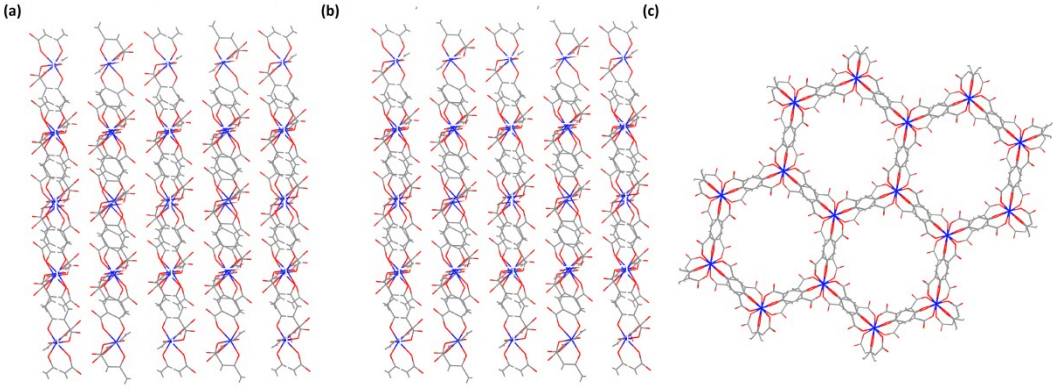


**Figure S2**. X-ray single crystal structure of **NTU-9** along (a) a axis, (b) b axis and (c) c axis

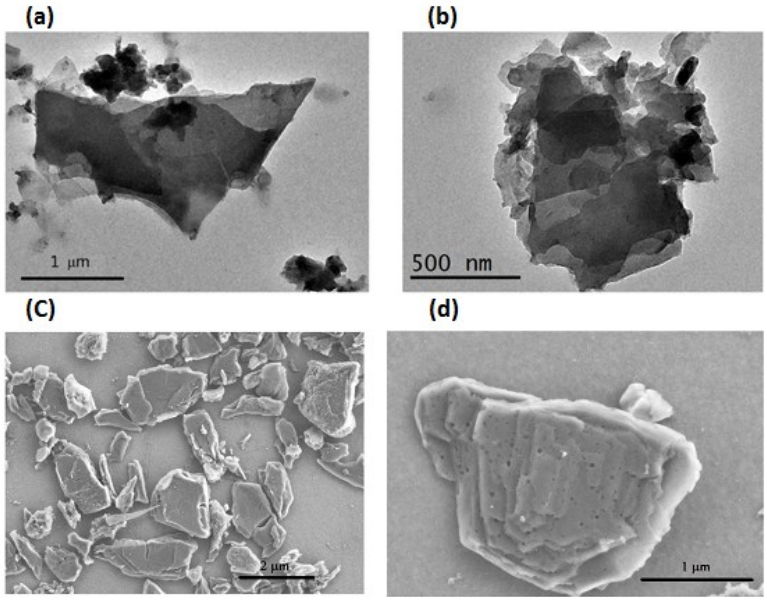


**Figure S3** TEM (a),(b) and SEM (c),(d) images of **NTU-9-NS**.

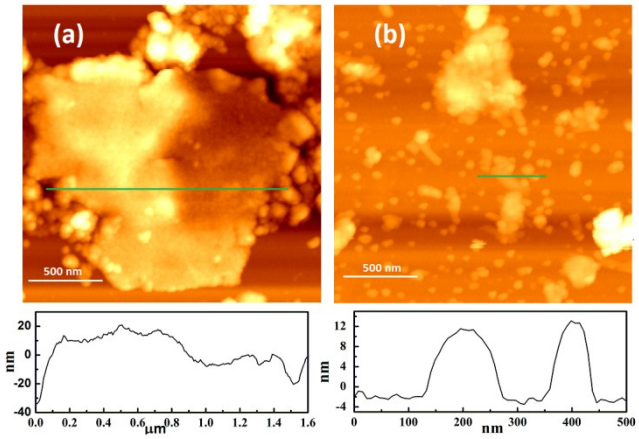


**Figure S4.** AFM images and the corresponding thickness of NTU-9-NS.

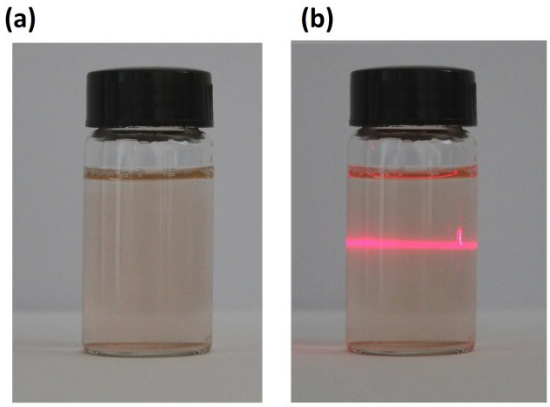


**Figure S5** Tyndall effect of a colloidal water suspension of **NTU-9-NS** nanosheets material.

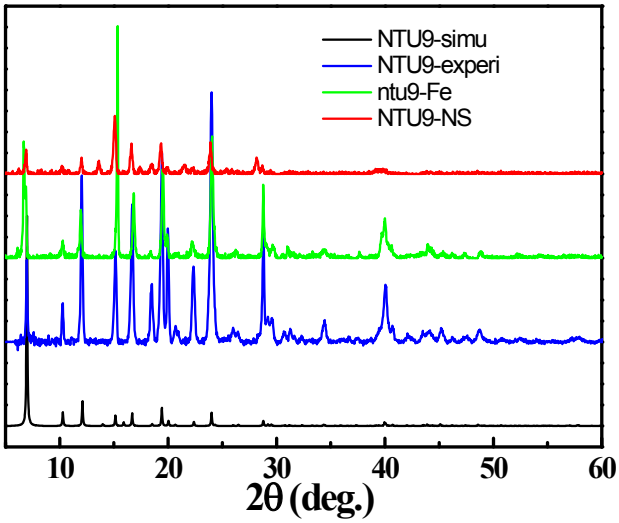


**Figure S6** Powder X-ray diffraction patterns of the as-synthesized **NTU-9-NS** nanosheets (before and after the addition of $Fe^{3+}$), bulk **NTU-9** and the one simulated from the X-ray single structure of **NTU-9**.

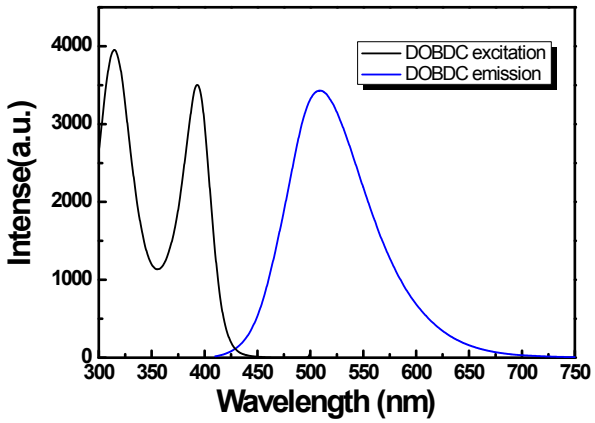


**Figure S7** The excitation (black) and PL spectra (blue) of the ligand DOBDC, monitored and excited at 510 nm and 390 nm, respectively.

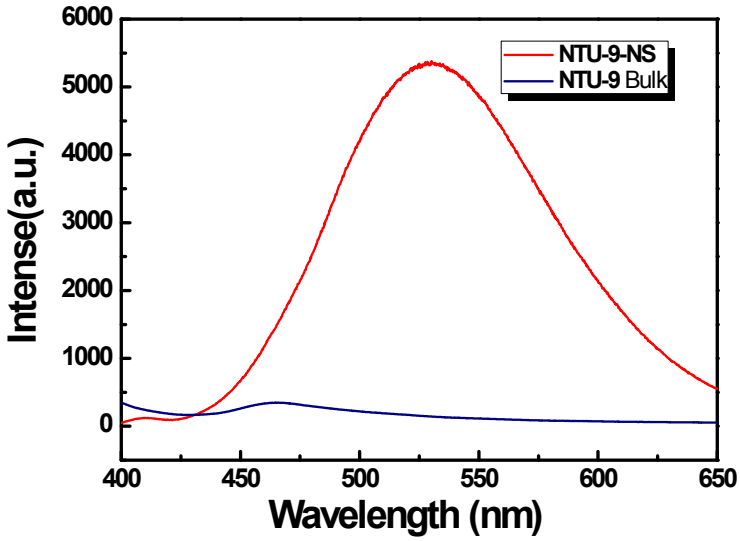


**Figure S8** The comparison of the PL spectra of **NTU-9-NS** nanosheet (red) in water solution and **NTU-9** bulk powder (navy), excited at 390 nm.

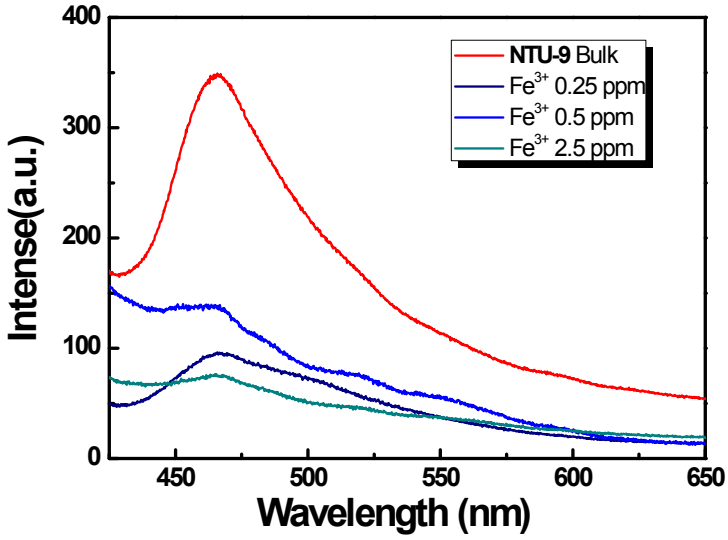


**Figure S9** PL spectra of **NTU-9** bulk powder with different amount of $Fe(NO_3)_3$.

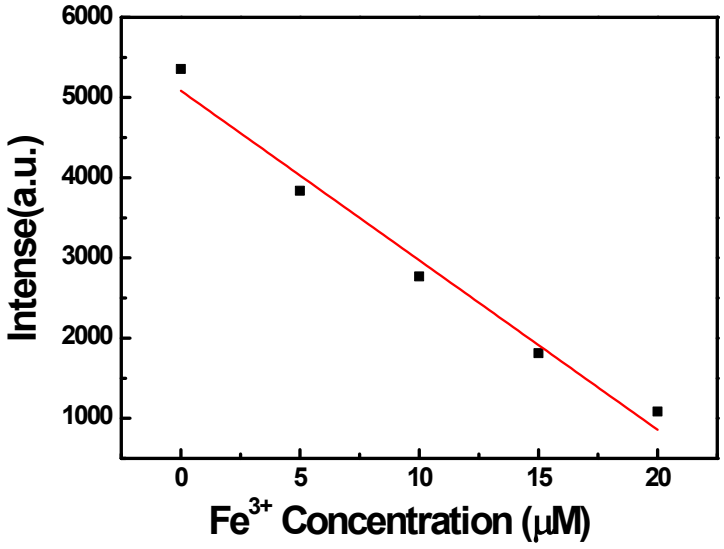


**Figure S10** The fitting curve of the emission intensity (530 nm) of **NTU-9-NS** vs. $Fe^{3+}$concentration (linear range 0-20 μM).

Linear Equation: Y = -211.4 X + 5084.8  R = 0.97497

S = $2.11 \times 10^8$ $M^{-1}$;

$S_b = \sqrt{\frac{\sum (I_0 - I_a)^2}{(N-1)}}$ =32.00 (N = 8)

LOD = $3S_b/S$ = 0.45 μM.

S is the slope of the calibration curve; $S_b$ is the standard deviation for replicating detections of blank solutions; $I_0$ is the fluorescence intensity of **NTU-9-NS** in water; $I_a$ is the average of the $I_0$.[2]

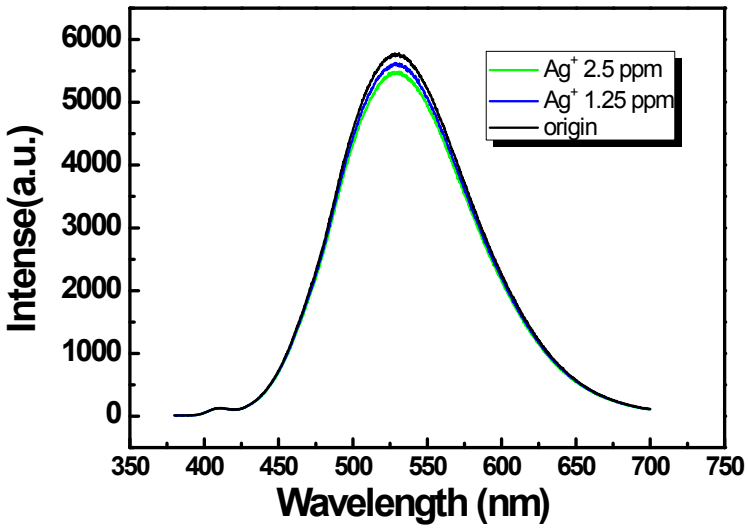


**Figure S11** The PL spectra of NTU9-NS with the addition of different concentration of $AgNO_3$, excited 390 nm.

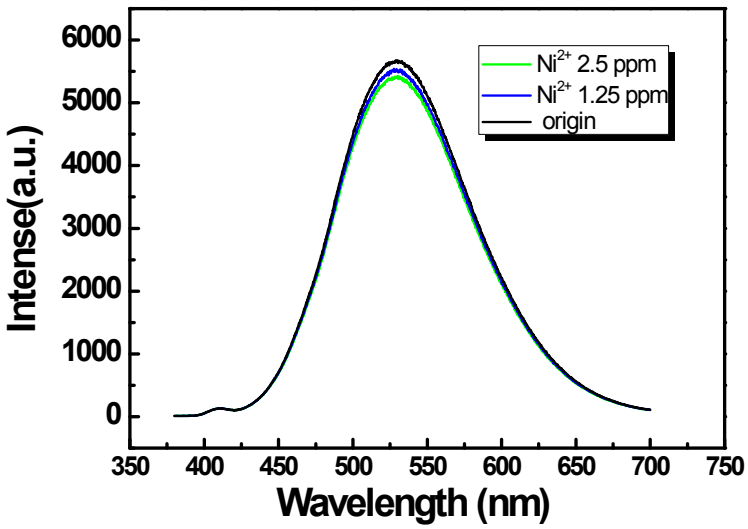


**Figure S12** The PL spectra of **NTU9-NS** with the addition of different concentration of $Ni(NO_3)_2$, excited 390 nm.

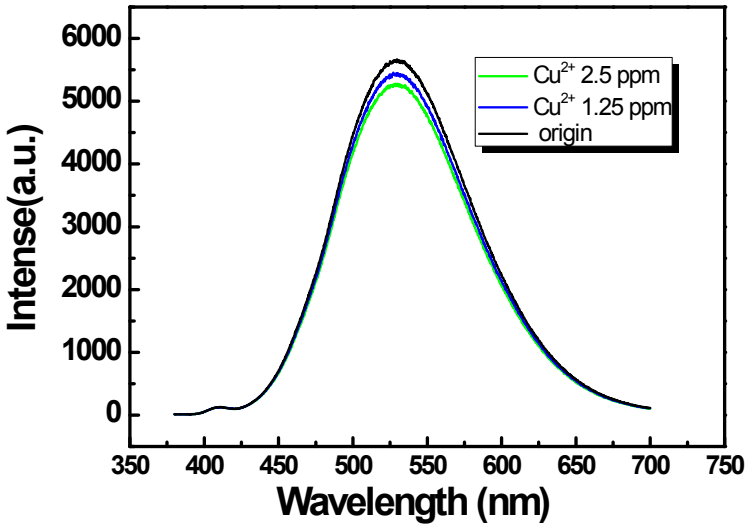


**Figure S13** The PL spectra of **NTU9-NS** with the addition of different concentration of $Cu(NO_3)_2$, excited 390 nm.

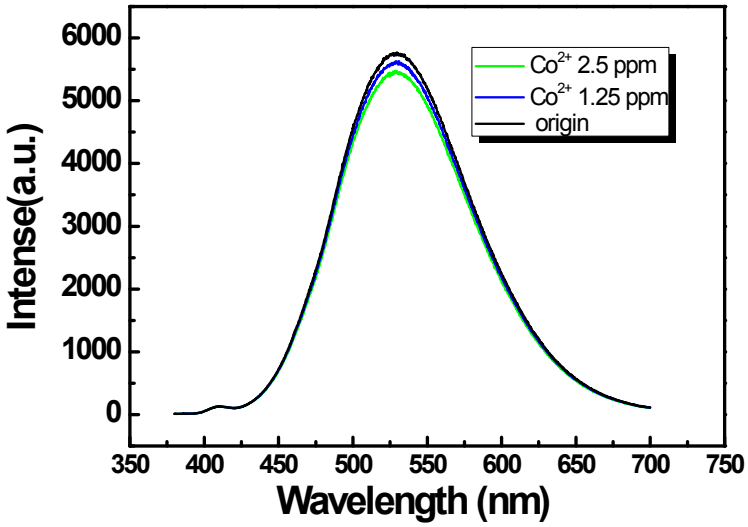


**Figure S14** The PL spectra of **NTU9-NS** with the addition of different concentration of $Co(NO_3)_2$, excited 390 nm.

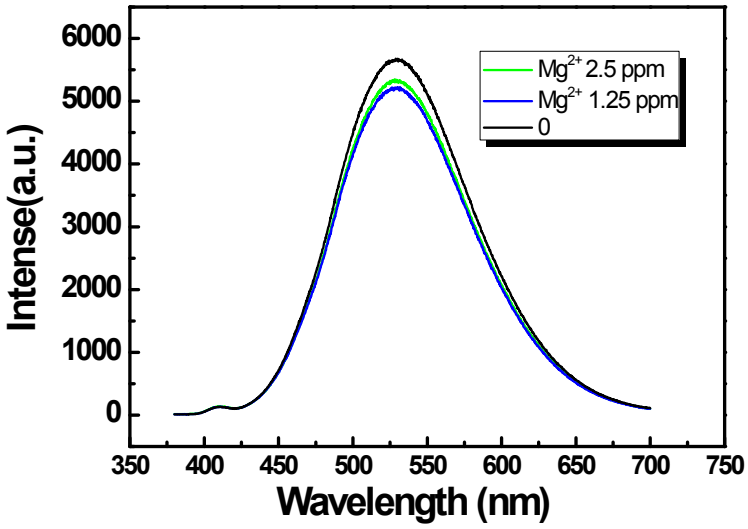


**Figure S15** The PL spectra of **NTU9-NS** with the addition of different concentration of $Mg(NO_3)_2$, excited 390 nm.

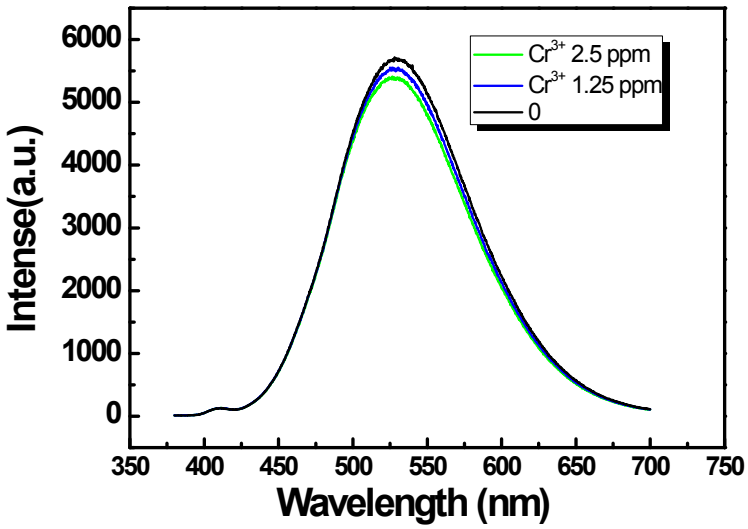


**Figure S16** The PL spectra of **NTU9-NS** with the addition of different concentration of $Cr(NO_3)_3$, excited 390 nm.

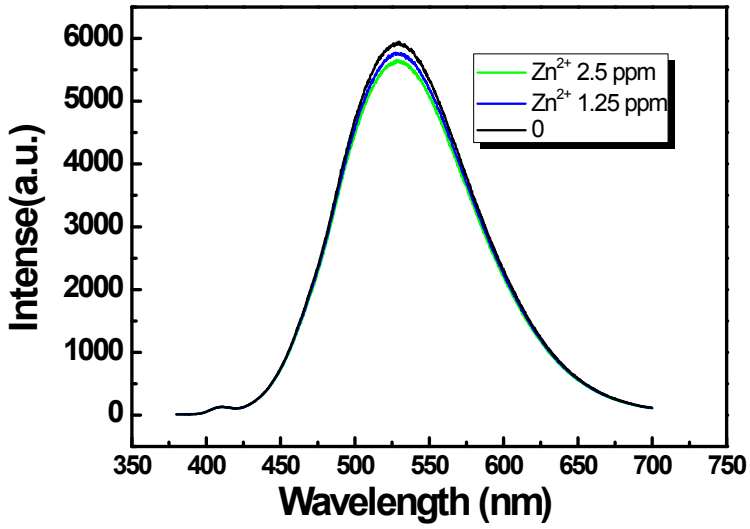


**Figure S17** The PL spectra of **NTU9-NS** with the addition of different concentration of $Zn(NO_3)_2$, excited 390 nm.

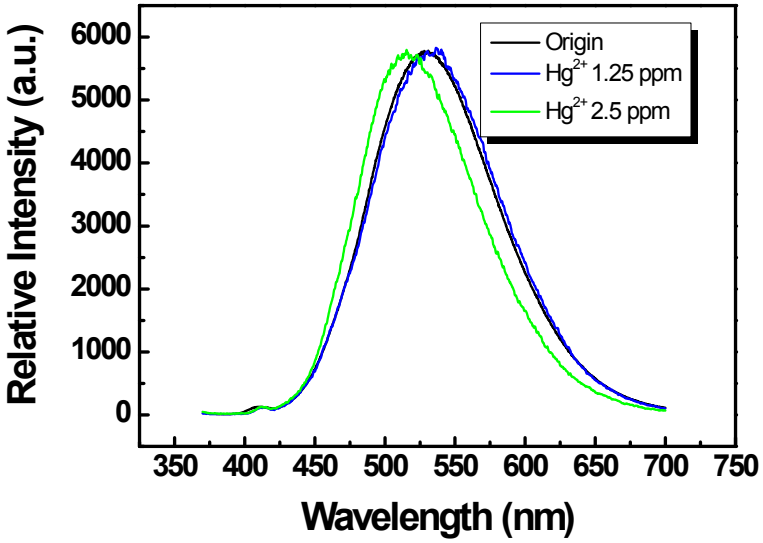


**Figure S18** The PL spectra of **NTU9-NS** with the addition of different concentration of $Hg(NO_3)_2$, excited 390 nm.

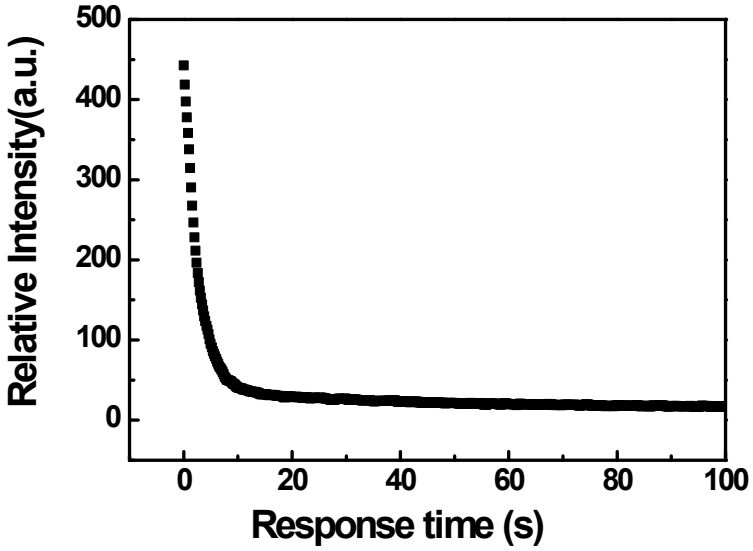


**Figure S19** Variation of fluorescence intensity of **NTU9-NS** at 530 nm with time after the addition of 2.5 ppm $Fe^{3+}$, excited 390 nm.

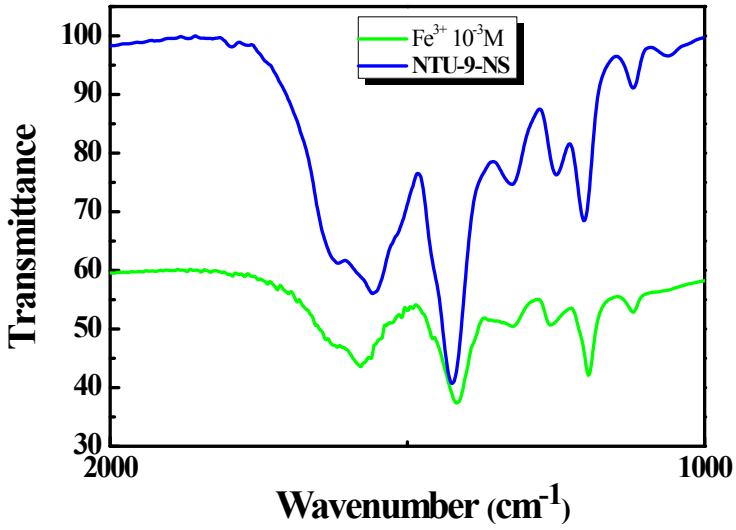


**Figure S20** The FT-IR of **NTU9-NS** nanosheets before and after the addition of $10^{-3}$M of $Fe^{3+}$**.**

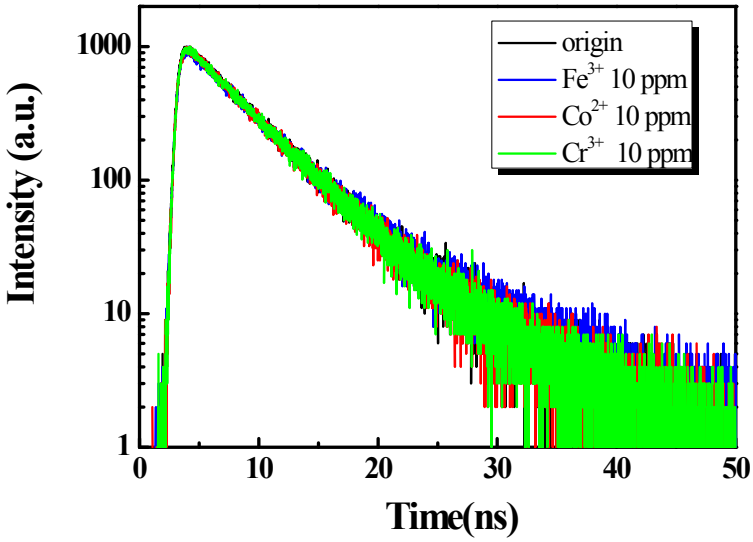


**Figure S21** PL decay curves of **NTU9-NS** in water solution with the addition of 10 ppm different metal ions (excited: 370 nm; monitored: 550 nm)

**Table S1** Fluorescence lifetime of origin water solution of **NTU9-NS** nanosheets and this solution with the different metal ions of 10 ppm (excited: 370 nm; monitored: 550 nm)

| Metal ions | $\tau_1$ (ns) |
|---|---|
| origin | 4.78 |
| $Fe^{3+}$ | 4.94 |
| $Co^{2+}$ | 6.44 |
| $Cr^{3+}$ | 4.80 |
| $Ag^{+}$ | 4.90 |
| $Zn^{2+}$ | 4.93 |
| $Ni^{2+}$ | 4.92 |
| $Mg^{2+}$ | 4.80 |
| $Cu^{2+}$ | 4.86 |

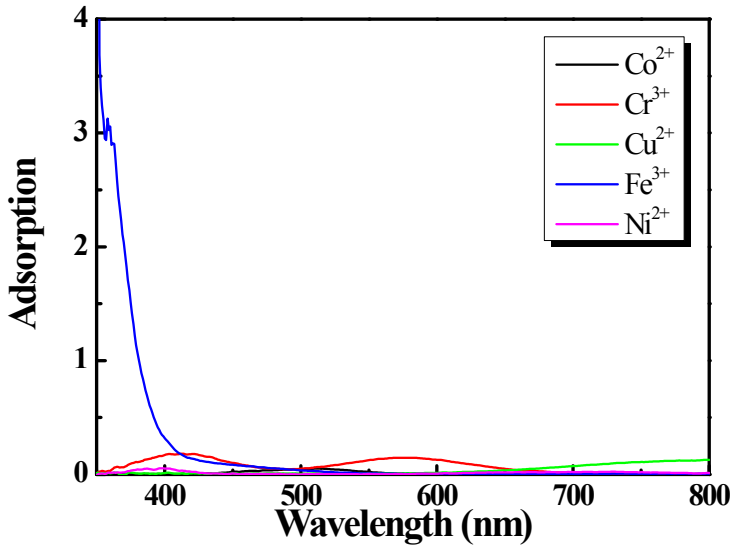


**Figure S22** UV-Vis spectra of different metal ions with the same concentration ($10^{-4}$M).

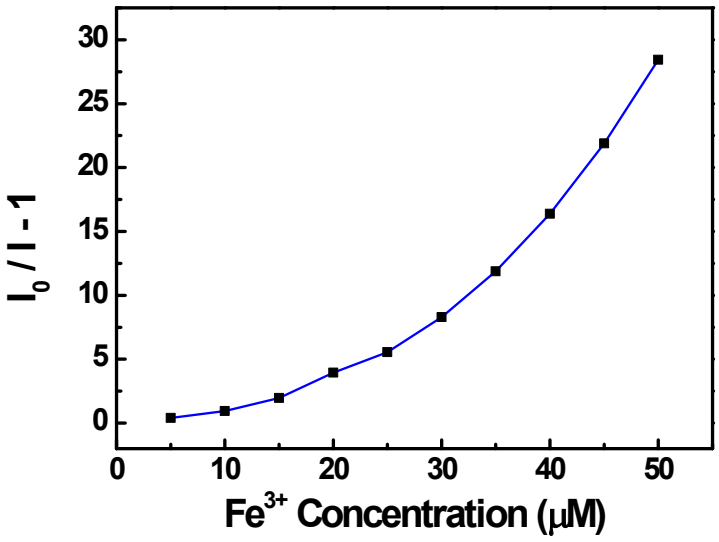


**Figure S23** The plot of ($I_0$/I-1) versus $Fe^{3+}$ concentration.

**Table S2** The outer electronic structure of different metal ions.

| Metal ions | Outer electronic structure |
|---|---|
| $Mg^{2+}$ | $2s^22p^6$ |
| $Zn^{2+}$ | $3d^{10}$ |
| $Hg^{2+}$ | $5d^{10}$ |
| $Ag^{+}$ | $4d^{10}$ |
| $Cr^{3+}$ | $3d^{3}$ |
| $Ni^{2+}$ | $3d^{8}$ |
| $Co^{2+}$ | $3d^{7}$ |
| $Cu^{2+}$ | $3d^{9}$ |
| $Fe^{3+}$ | $3d^{5}$ |

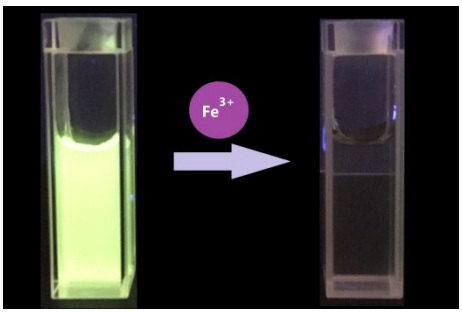


**Figure S24** The luminescent quenching photo of NTU-9-NS with the addition of $Fe^{3+}$.

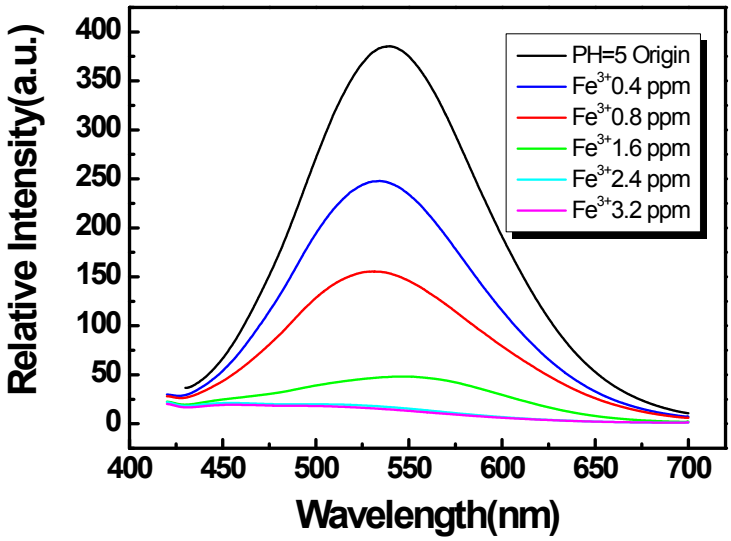


**Figure S25** The PL spectra of **NTU9-NS** at PH=5 with the addition of different concentration of $Fe^{3+}$, excited 390 nm.

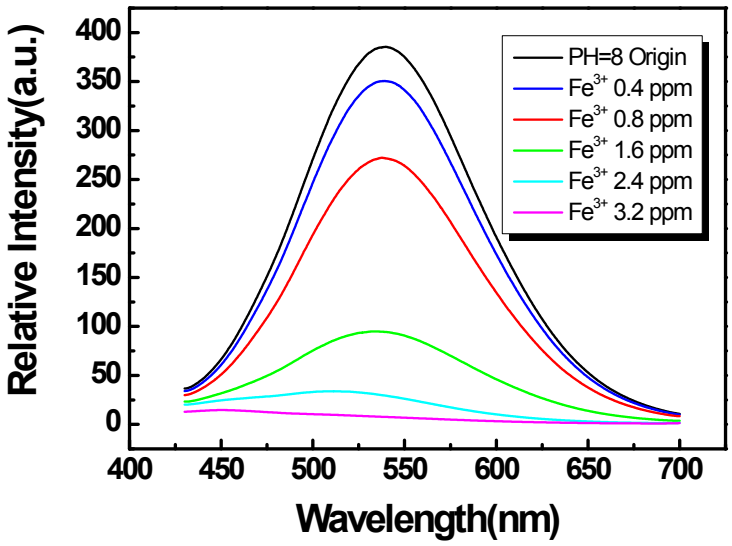


**Figure S26** The PL spectra of **NTU9-NS** at PH=8 with the addition of different concentration of $Fe^{3+}$, excited 390 nm.